metals

MDPI

Article

Predicting the Macroscopic Shear Strength of Tightened-Bonded Joints from the Intrinsic High-Pressure Properties of Anaerobic Adhesives

Davide Castagnetti [1], Pasqualino Corigliano [2,*], Calogero Barone [1], Vincenzo Crupi [2], Eugenio Dragoni [1] and Eugenio Guglielmino [2]

[1] Department of Sciences and Methods for Engineering, University of Modena and Reggio Emilia, Via G. Amendola 2, 42122 Reggio Emilia, Italy; davide.castagnetti@unimore.it (D.C.); calogero.barone@plastitaliaspa.com (C.B.); eugenio.dragoni@unimore.it (E.D.)
[2] Department of Engineering, University of Messina, Contrada di Dio-98166–Sant'Agata, 98166 Messina, Italy; crupi.vincenzo@unime.it (V.C.); eguglie@unime.it (E.G.)
* Correspondence: pcorigliano@unime.it

Abstract: This scientific study aims to validate the applicability of a micromechanical model for predicting the static shear strength of hybrid interfaces that are pressure-reinforced and bonded with anaerobic adhesives. To identify the parameters for the micromechanical model, a systematic experimental test plan involving high-strength steel butt specimens bonded with anaerobic adhesive in a finite thickness was performed. The experimental investigation was based on torque tests, which provided the shear strength of two anaerobic adhesives subjected to different values of contact pressure, ranging from 0 up to 1000 MPa. Based on the intrinsic high-pressure properties of the finite-layer adhesives, the formerly developed micromechanical model of hybrid interfaces satisfactorily predicted the macroscopic strength of tightened-bonded joints taken from the literature.

Keywords: anaerobic adhesives; finite thickness; micromechanical model validation; experimental torque tests

Citation: Castagnetti, D.; Corigliano, P.; Barone, C.; Crupi, V.; Dragoni, E.; Guglielmino, E. Predicting the Macroscopic Shear Strength of Tightened-Bonded Joints from the Intrinsic High-Pressure Properties of Anaerobic Adhesives. *Metals* **2022**, *12*, 1141. https://doi.org/10.3390/met12071141

Academic Editor: Xiangdong Gao

Received: 30 May 2022
Accepted: 30 June 2022
Published: 4 July 2022

1. Introduction

Although welding remains the main joining technique for metallic materials, the application of adhesive joints is increasingly showing potential[1,2]. Welding is used in shipbuilding for connecting ship structures [3] and also for connecting dissimilar metal parts of structure and superstructure by means of dissimilar welded joints [4]. However, welding techniques cannot always be employed, and the use of adhesives is crucial. Typical applications of anaerobic adhesives are mechanically tightened metal joints, where these thermosetting acrylic polymers can improve strength over the purely frictional dry interface.

The use of adhesives ranges from automotive and off-road vehicles to railway and marine fields or any industrial case where bolted joints, flanged couplings, and interference fits must ensure high strength and reliability [5].

Regarding marine applications, environmental attacks, due to different factors (i.e., water, temperature), can degrade structural adhesive joints. As reported by Myslick et al., underwater joining by adhesive bonding represents an innovative approach and underwater glued stud bonding fasteners for offshore structures were investigated [6]. Adhesive joints are increasingly being used in shipbuilding, but their application requires better knowledge of their mechanical properties and durability within a hostile environment, such as those faced by ships.

Specifically, anaerobic adhesives cure in the absence of air and/or by means of metal contact, filling bond gaps from 0.025 mm to ~1 mm. They are less toxic than other acrylics, and they do not produce corrosion to metals. Advantages also include cure-on-demand functionality, low odour levels, single-part room temperature curing and high levels of durability, thanks to their tolerance to organic solvents and water, weathering, and temperatures of up to about 200 °C [7]. Anaerobic adhesives can be applied to structural bonds, principally with materials such as metals and glass and, to a minor extent, wood, and plastics. Within this context, anaerobic adhesives could represent a new frontier in metal joining in the marine industry [7].

Currently, anaerobic adhesives find several applications in the marine field [5] including the securing of steering mechanisms, raw material processing for propeller hubs, end cap fixings on hub shafts, and securing dowel pins in propeller blades, as displayed in Figure 1.

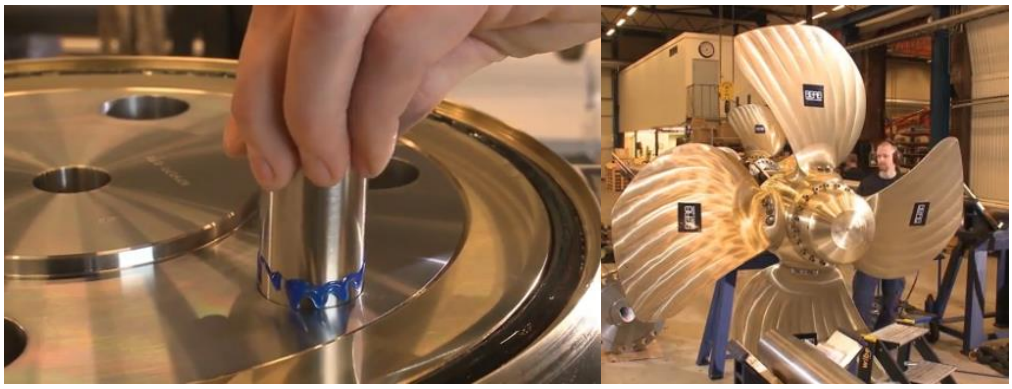

Figure 1. Typical application of anaerobic adhesives in propeller blades (securing dowel pins in propeller blades and thread lockers).

In the technical literature, many researchers investigate the mechanical response of anaerobic adhesives.

Several types of steel and aluminium structures glued by means of adhesive are analysed by the authors of [8]. Hybrid joints involving the manufacturing procedure for adhesively bonded K-joints used in offshore structures are proposed in [9].

Romanos [10] evaluated the static and fatigue strength of friction-bonded interfaces. Yoneno et al [11] examined the interface stress distribution of bonded shrink-fitted joint under push-off force. Dragoni and Mauri [1] investigated the contributions given by friction and adhesive to the overall strength of an annular friction-bonded interface. Sekercioglu [12–14] analysed which factors affect the static and dynamic strength of adhesively bonded cylindrical components. Mengel et al. [15] showed the beneficial effect that hydrostatic pressure has on adhesive (during the curing process) concerning the strength of the joint. Aronovich et al. [16] and Sineokov et al. [17] focused on the curing mechanisms of anaerobic adhesives. Croccolo et al. [18–24] evaluated: the strength of adhesively bonded interference fit under both static and dynamic excitation, the effect of temperature, the effect of the engagement ratio for pin-collar joints, and the improvements in threaded connections thanks to the application of anaerobic adhesives on different materials and configurations. Oinonen et al. [25–27] focused on the static and fatigue shear strength of epoxy adhesives in steel interfaces. Kleiner and Fleischmann [28] provided a summary of technologies for threadlocking and interference-fit adhesive joints. Gallio et al. [29] the contribution of adhesives concerning the interference on the performance of hybrid joints and press-fitted and bonded joints. Abdel [30] presented a literature review on fatigue in adhesively bonded joints, including anaerobic adhesives, noting that only a few works from other authors have dealt with the shear strength of hybrid friction-bonded interfaces [18,31–33].

This literature review highlights the lack of a clear constitutive model able to predict the shear strength of hybrid interfaces press-fitted and bonded with anaerobic adhesive, as a function of the type of adhesive, of the adherends, and the contact pressure applied. In addition, relatively low values of contact pressure were investigated experimentally. Thus, one of the objectives of this paper is to extend, apply, and validate a micromechanical model to higher contact pressures by means of experimental torque tests.

According to the results of a systematic test plan, Dragoni and Mauri [1,2] proposed a micromechanical model able to assess the shear strength of the hybrid interface.

This model assumes piezoresistive behaviour of the adhesive, specifically:

-the adhesive filling the voids around the protrusions of the mating surfaces, which at zero contact pressure, exhibits its intrinsic shear strength;

-by contrast, the adhesive exposed to high contact pressure between the crests of the mating surfaces remarkably improves its shear strength [34–38].

More recent experimental and numerical investigations by Castagnetti et al. [39–42] preliminarily confirmed the applicability of this model.

On the basis of a systematic experimental test plan, which measured the shear strength of the joint up to complete failure, Castagnetti et al. [42,43] proposed a simple constitutive model combining a cohesive law and a pure friction law that describes the post elastic behaviour of the hybrid interface.

To assess the hypothesis of piezoresistive behaviour of the thin adhesive proposed by Dragoni and Mauri [2], Corigliano et al. [44] investigated how to measure the shear strength of an anaerobic adhesive layer with a finite thickness and surface area, subject to nearly uniform contact pressure, up to 1000 MPa. Specifically, they focused on the test bench setup and specimen preparation and validation, also performing a full-field strain measurement through Digital Image Correlation (DIC).

This scientific study completes this preliminary experimental investigation with the aim of validating the capability of the micromechanical model proposed by Dragoni et al. [2] in predicting the static shear strength of hybrid interfaces, pressure-reinforced and bonded with anaerobic adhesives.

To identify the parameters for the micromechanical model, a systematic experimental test plan involving high-strength steel specimens made of two adherends bonded head-to-head on an annular surface, was performed.

The experimental investigation was based on torque tests, which provided the shear strength of the anaerobic adhesive in a finite thickness and surface area, with contact pressure ranging from 0 up to 1000 MPa, both for a weak (Loctite 243) and a strong (Loctite 638) anaerobic adhesive.

Based on the intrinsic shear strength vs. the pressure properties of the adhesive in finite layers, the formerly developed micromechanical model of hybrid interfaces was able to satisfactorily predict the macroscopic strength of tightened-bonded joints taken from the literature [1,2].

2. Micromechanical Model

2.1. Assumptions

As described in Figure 2, the model condenses the roughness of the contacting surfaces into two protrusions that face each other over a fraction, A_r, of the nominal contact area, A.

According to the model, the adhesive fills the voids all around the protrusions, where it receives no pressure, and forms a thin layer between the protrusions, subject to the yield pressure, Y, of the softest adherend.

Based on the typical response of polymeric materials, the shear strength of the adhesive τ_a under an effective contact pressure p, can be written as [1,2]:

$$\tau_a(p) = \tau_{a0} + \Delta\tau_{ap}(p) \quad (1)$$

where $\Delta\tau_{ap}$ is the shear strength increment of the adhesive at a given pressure, p, and τ_{a0} is the unit shear strength of the adhesive at zero pressure.

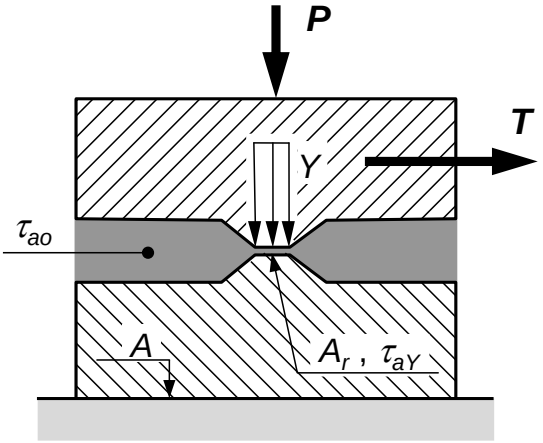

Figure 2. Schematic representation of the hybrid interface according to the micromechanical model.

2.2. Theory

According to the micromechanical model, the shear failure load of the joint amounts to:

$$T = \tau_{a0}\, A + \, (\tau_{aY} - \tau_{a0})\, P/Y = T_0 + T_Y \tag{2}$$

where:

τ_{aY} is the shear strength of the adhesive under a pressure Y (i.e., $\tau_a(Y) = \tau_{a0} + \Delta\tau_{ap}(Y)$);

A is the nominal area of contact;

$T_0 = \tau_{a0}\, A$ is the constant term of the shear failure load;

$T_Y = (\tau_{aY} - \tau_{a0})\; P/Y$ is the variable term of the shear failure load.

In case the shear strength of the adhesive is directly proportional to the effective contact pressure p, it follows that:

$$\Delta\tau_{ap}(p) = \alpha\, p \tag{3}$$

Hence, for an effective contact pressure equal to the yield strength of the adherends, Y, it follows that:

$$\Delta\tau_{ap}(Y) = \alpha\, Y \tag{4}$$

which turns Equation (1) into the following:

$$\tau_{aY} = \tau_a(Y) = \tau_{a0} + \alpha\, Y \tag{5}$$

thus, the shear failure load of the joint (Equation (2)) becomes:

$$T = \tau_{a0}\, A + \, (\alpha\, Y + \, \tau_{a0} - \tau_{a0})\, P/Y \tag{6}$$

$$T = \tau_{a0}\, A + \, (\alpha\, Y)\, P/Y \tag{7}$$

$$T = \tau_{a0}\, A + \, \alpha P \tag{8}$$

In conclusion, assuming that the relationship between the shear strength and the applied pressure on the adhesive is linear, the shear failure load of the joint is independent of the adherend material properties.

The main aim of this work is to find out the true form of relationship (1) and check whether it can be reduced to a linear form, leading to Equation (2).

3. Materials and Methods

3.1. Adherends

Figure 3 shows the geometry of the specimen used in the test plan, corresponding to the one used by Corigliano et al. [44]. Two cylindrical adherends, manufactured from a Ø22H7 ground bar made of quenched and tempered high strength steel, 39NiCrMo3, were bonded end-to-end on an annular surface. The specimens were of the same material batch used by Corigliano et al. [44], thus having the same material properties (Rs = 992 MPa and R = 995 MPa).

To reproduce the microscale configuration of a thin adhesive film bearing high pressure, like the one trapped between the surface protrusions in Figure 1, a 0.1 mm thickness for the adhesive layer in the specimen was chosen. According to simple geometrical analysis, this thickness value, combined with a surface roughness equal to 1.0 μm or lower, gives a configuration where the roughness of the adherends is negligible compared to the finite thickness of the adhesive layer; thus, this configuration reproduces in the macroscale the microscale condition of a thin adhesive layer, bearing a high and uniform pressure over the whole surface area of the adhesive [44].

The preparation of the bonding surface of the adherends started with sandpaper, followed by degreasing via Loctite 7063, and finally the roughness of the surface was measured. Figure 3 also shows a picture of an adherend after preparation. A weak (Loctite 243 [45]) and a strong (Loctite 638 [46]) anaerobic adhesive were investigated.

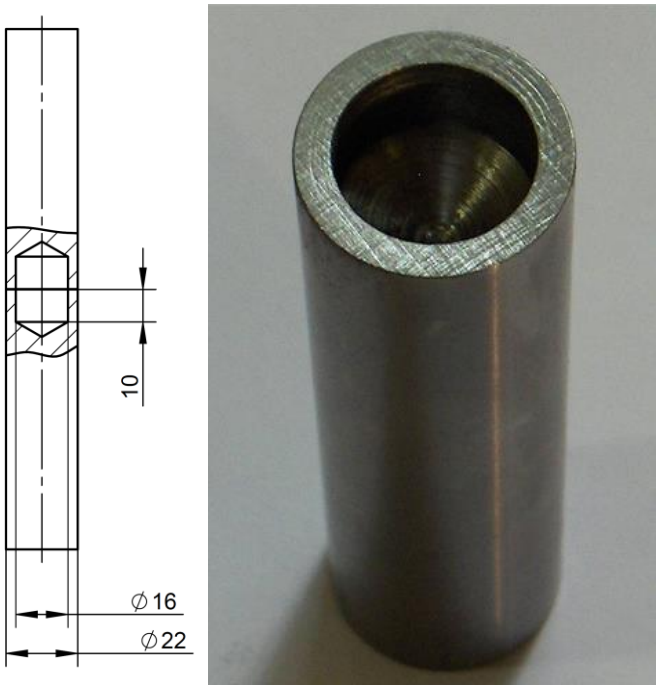

(**a**) (**b**)

Figure 3. (**a**): Geometry of the bonded specimen (units in mm), and (**b**): picture of an adherend after preparation.

3.2. Test Bench and Test Procedure

The tests were executed on a bi-axial 8854 Instron machine, with a load cell of 250 kN and a maximum torque of 2 kNm.

Firstly, the adherends were setup on the top and bottom fixture. Secondly, the top adherend was slowly brought towards the bottom one until contact with zero pressure: this position was registered as zero strokes. Thirdly, the top adherend was raised up to allow adhesive application on the annular surface of the bottom adherend. Fourthly, the top adherend was slowly brought towards the bottom one, up to a 0.1 mm gap from the

zero strokes previously registered. According to the curing conditions suggested by Murokh [16] and Sineokov [17], the joint region with a thin aluminium sheet was wrapped in order to ensure electrical continuity between the top and bottom adherend.

The polymerization of the hybrid interface lasted 6 h at 45 °C, which was a temperature originated by the servo-hydraulic test machine; at the end, we removed the aluminium sheet. The test applied the prescribed axial preload in a time period equal to 120 s, followed by a quasi-static relative rotation between the adherends, at a speed of 0.2°/s, up to complete failure of the joint.

Figure 4 shows a picture of the setup of a specimen on the test machine.

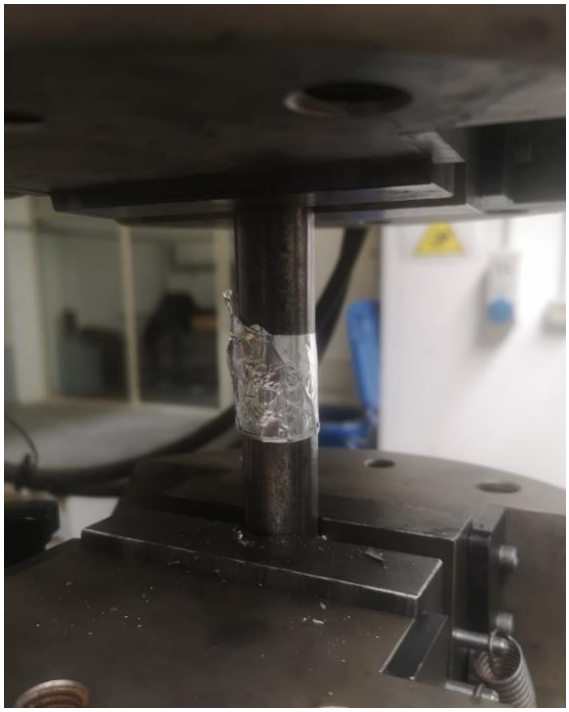

Figure 4. Picture of a specimen on the test machine.

3.3. Test Plan

The test plan investigated two variables. Firstly, the adhesive type: a weak (Loctite 243 [45]) and a strong (Loctite 638 [46]) anaerobic adhesive in addition to a dry contact condition. Secondly, the nominal contact pressure between the adherends over five levels: 0 MPa, 250 MPa, 500 MPa, 750 MPa, and 1000 MPa (see Table 1).

Table 1. Variables of the test plan.

Variables	**Levels**				
Adhesive Type	**Loctite 243**		**Loctite 638**	**Dry Contact**	
Nominal contact pressure (MPa)	0	250	500	750	1000

These contact pressure levels allow for the investigation of the response of the adhesive over a wide range of conditions experienced in real applications, e.g., zero pressure corresponding to a joint without any mechanical tightening or to the adhesive filling the voids between the mating protrusions of the adherends, and non-zero pressure corresponding to clamped fitted and bonded joints.

The test plan involved five replications for each experimental configuration, with the exception of the dry contact condition for which no replications were performed, for a total of 50 tests.

4. Results

4.1. Test Results

A typical torque-rotation curve obtained for the Loctite A 638 adhesive with a contact pressure of 1000 MPa is shown in Figure 5. The first failure of the Loctite A 638 adhesive is observed via the strong decrease in torque (at about 5°), which is also accompanied by partial plastic strain in the adherends. The subsequent torque transmitted after the adhesive failure is due to the friction between the two adherends, mediated by the residual adhesive layer.

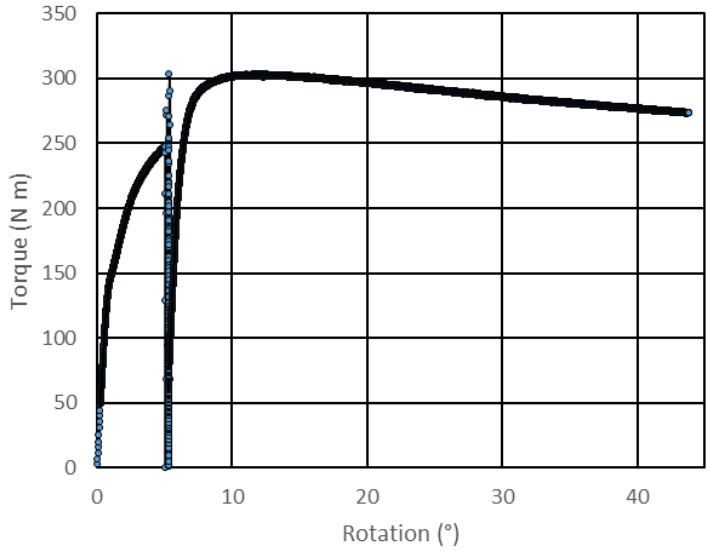

Figure 5. Torque-rotation curve obtained for the Loctite A 638 adhesive with a contact pressure of 1000 MPa.

For all the test configurations of the test plan, Table 2 presents the values of the failure torque of the joints, retrieved from the experimental torque-rotation curves.

Table 2. Experimental failure torque.

Nominal Contact Pressure	Failure Torque (Nm)		
(MPa)	243	638	Dry Contact
0	46.7	51.2	0.0
0	8.1	40.1	-
0	-	54.1	-
0	-	63.1	-
0	-	44.2	-
250	65.6	140.0	92.9
250	70.9	120.0	-
250	84.4	151.0	-
250	32.0	120.0	-
250	33.0	152.6	-
500	110.5	210.0	124.6
500	93.3	229.0	-
500	122.7	237.0	-
500	76.0	213.0	-
500	68.0	223.0	-
750	154.4	291.5	184.8
750	141.4	285.7	-

750	140.9	300.0	-
750	132.0	296.0	-
750	138.0	300.0	-
1000	151.4	336.0	229.1
1000	192.4	-	-
1000	159.3	-	-
1000	149.0	-	-
1000	-	-	-

The test results in Table 2 highlight that some data are missing, specifically for the Loctite 638 adhesive at a nominal contact pressure of 1000 MPa. This was a consequence of an experimental problem; given the high strength of the adhesive and the high torque at failure, the collapse of the bonded joint causes the release of a large amount of elastic energy from the specimen, with strong dynamic oscillations on the load cell, thus preventing the registration of a representative value of the failure torque.

The shear strength τ_r was calculated according to the following relationship:

$$\tau_r = \frac{16M_t}{\pi(D^2 - d^2)(D + d)} \quad (9)$$

where M_t is the applied torque, D is the external diameter of the adherend, and d is the diameter of the inner hole.

Figure 6 shows the shear strength as a function of the contact pressure registered in the experimental test plan for all the investigated configurations. The solid red triangles refer to Loctite 243. The solid blue squares refer to Loctite 638. The black crosses refer to a dry interface. The dashed lines are the linear regression of the corresponding points.

Table 3 presents the coefficients of the linear regression lines in Figure 6, corresponding to the micromechanical model (Equation (2)).

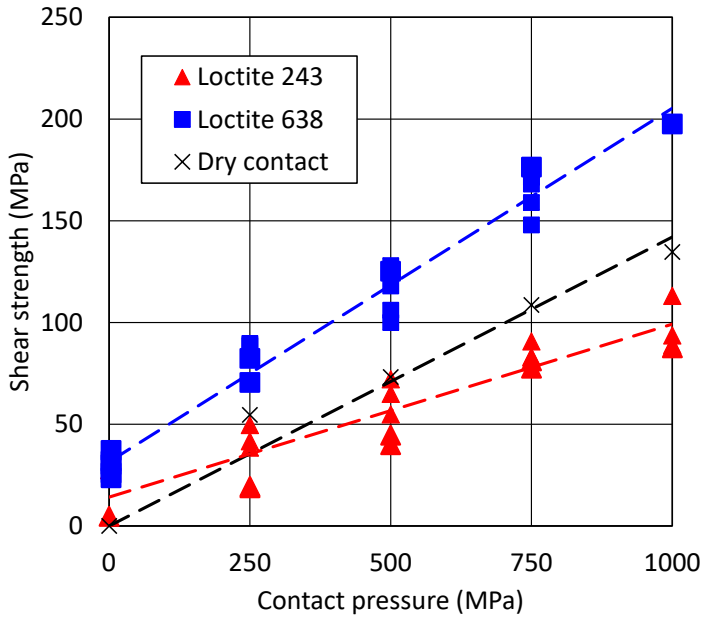

Figure 6. Shear strength as a function of the nominal contact pressure.

Table 3. Coefficients of the linear regression lines for both adhesives and dry contact.

Adhesive Type	Loctite 243	Loctite 638	Dry Contact
τ_{a0} (MPa)	14.16	31.58	0
α	0.0851	0.1738	0.1421

4.2. Model Evaluated in the Present Study and Validation with Collected Literature Results on Hybrid Joints

In order to validate the applicability of the micromechanical model in the prediction of real hybrid interfaces press-fitted and bonded with anaerobic adhesives, literature data from Dragoni and Mauri [1,2], Castagnetti and Dragoni [40,42], Ragni et al. [43] were retrieved. All these experimental data refer to anaerobic adhesive in a thin film, as this usually occurs in real industrial applications.

Figures 7 and 8 show the comparison between the obtained micromechanical model predictions by means of Equation (1) using the parameters reported in Table 3, according to the results of the present investigations reported in Figure 6, with respect to the data from the literature for the Loctite 243 and the Loctite 648 adhesives, respectively.

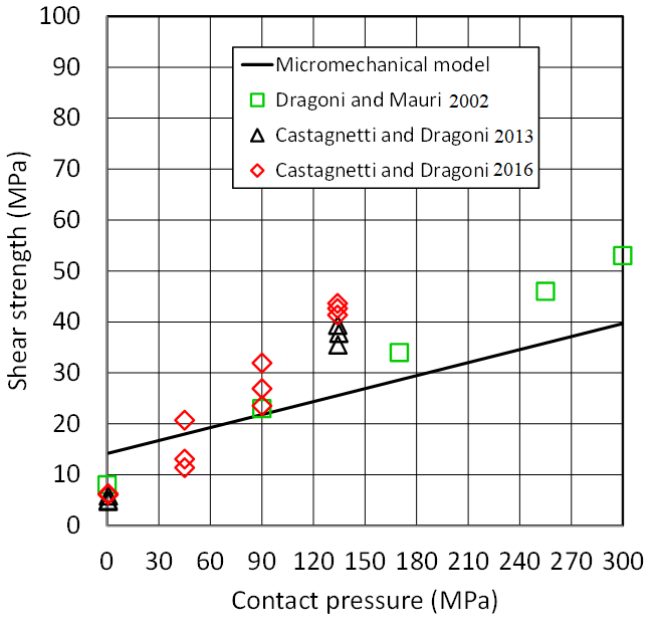

Figure 7. Comparison between the computational model prediction and experimental data from the literature [2,40,42] for the Loctite 243 adhesive.

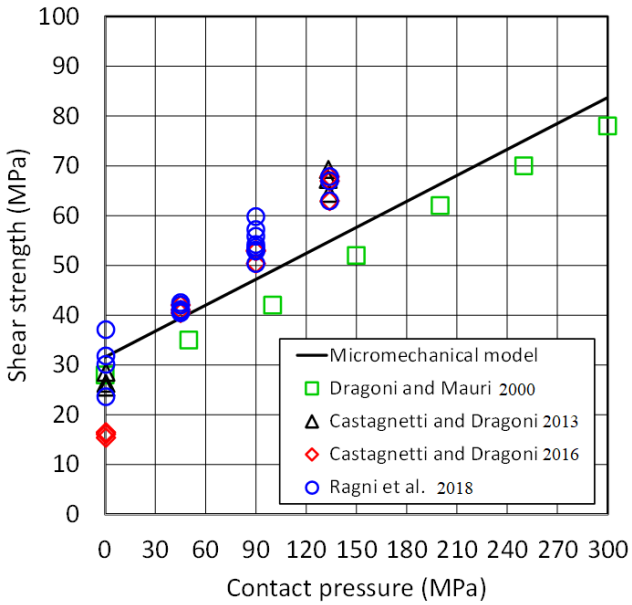

Figure 8. Comparison between the computational model prediction and experimental data from the literature [1,40,42,43] for the Loctite 638 adhesive.

5. Discussion

For both adhesives, the shear strength values as a function of the nominal contact pressure in Figure 6 show the typical scatter of these types of tests.

It is worth noting that both adhesives clearly exhibit a linear dependence between the shear strength and the applied contact pressure; as Table 3 clearly shows, the strong anaerobic adhesive (Loctite 638) has a shear strength at zero pressure (τ_{a0}) and a coefficient of the linear term (α) that nearly doubles that of the weak anaerobic adhesive (Loctite 243). Specifically, Figure 6 shows that the shear strength of the weak anaerobic adhesive becomes lower than dry contact for nominal contact pressure higher than 250 MPa; this behaviour confirms the results of preliminary investigations [2,44] and underlines that, above a given contact pressure, the weak anaerobic adhesive acts as a lubricant compared to dry contact. By contrast, the strong anaerobic adhesive exhibits a higher slope than dry contact and a remarkably higher strength over the whole range of investigation.

The comparison between the micromechanical model prediction (Equation (1), according to the coefficients in Table 3) and the literature data shows good agreement, specifically with the data from Dragoni and Mauri [2]. With regard to Loctite 243, Figure 7 highlights that the micromechanical model prediction has a slightly lower slope than the data from Dragoni and Mauri [2], while a more significant difference appears between the micromechanical model prediction and the data from Castagnetti and Dragoni [40,42]. Specifically, the micromechanical model tends to overestimate the response at low contact pressure and underestimate it at high contact pressure. This may be imputed to an effect of the adherends material that the micromechanical model neglects.

In Figure 8, we can observe a similar scenario, but with closer agreement; for the strong anaerobic adhesive (Loctite 638), the micromechanical model exhibits a close agreement with the results from Dragoni and Mauri [1] despite a slight overestimation of the response of the joint. The comparison between the micromechanical model and more recent data from Castagnetti et al. [40,42] and Ragni et al. [43] highlights nearly the same value at zero pressure but with a higher slope of the test results compared to the micromechanical model prediction.

On the whole, this simple micromechanical model, which relies on two parameters only, appears to be a good tool for predicting the shear strength of structural joints bonded with anaerobic adhesives.

6. Conclusions

A systematic experimental test plan involving high-strength steel specimens made of two adherends, bonded head-to-head on an annular surface, was performed. The experimental investigation was based on torque tests, which provided the shear strength of the anaerobic adhesive in a finite thickness and surface area, with contact pressure ranging from 0 up to 1000 MPa, both for a weak (Loctite 243) and a strong (Loctite 638) anaerobic adhesive. Both adhesives clearly exhibit a linear dependence between the shear strength and the applied contact pressure, which allowed us to define the coefficients of the theoretical micromechanical model; the strong anaerobic adhesive (Loctite 638) has a shear strength at zero pressure (τ_{a0}) and a coefficient of the linear term (α) that nearly doubles that of the weak anaerobic adhesive (Loctite 243). The shear strength of the weak anaerobic adhesive becomes lower than dry contact for nominal contact pressure higher than 250 MPa, meaning that, above a given contact pressure, the weak anaerobic acts as a lubricant compared to dry contact.

Overall, this simple micromechanical model can predict the shear strength of structural joints bonded with anaerobic adhesives, taking into account only two parameters.

Author Contributions: Conceptualization, D.C, P.C., E.D., V.C. and E.G.; methodology, P.C., D.C. and V.C.; investigation, P.C. and C.B.; writing—review and editing, D.C., P.C., E.D. and V.C.; supervision, E.D., V.C. and E.G. All authors have read and agreed to the published version of the manuscript.

Funding: This research received no external funding.

Informed Consent Statement: Not applicable.

Data Availability Statement: Not applicable.

Conflicts of Interest: The authors declare no conflict of interest.

References

1. Dragoni, E.; Mauri, P. Intrinsic Static Strength of Friction Interfaces Augmented with Anaerobic Adhesives. *Int. J. Adhes. Adhes.* **2000**, *20*, 315–321. https://doi.org/10.1016/S0143-7496(99)00062-7.
2. Dragoni, E.; Mauri, P. Cumulative Static Strength of Tightened Joints Bonded with Anaerobic Adhesives. *Proc. Inst. Mech. Eng. Part L J. Mater.Des. Appl.* **2002**, *216*, 9–15.
3. Corigliano, P.; Crupi, V.; Pei, X.; Dong, P. DIC-Based Structural Strain Approach for Low-Cycle Fatigue Assessment of AA 5083 Welded Joints. *Theor. Appl. Fract. Mech.* **2021**, *116*, 103090. https://doi.org/10.1016/j.tafmec.2021.103090.
4. Corigliano, P.; Crupi, V.; Guglielmino, E. Non Linear Finite Element Simulation of Explosive Welded Joints of Dissimilar Metals for Shipbuilding Applications. *Ocean Eng.* **2018**, *160*, 346–353. https://doi.org/10.1016/j.oceaneng.2018.04.070.
5. Da Silva, L.F.M.; Pirondi, A.; Öchsner, A. *Hybrid Adhesive Joints*; Advanced Structured Materials; Springer: Berlin/Heidelberg, Germany, 2011; ISBN 9783642166235.
6. Myslicki, S.; Kordy, H.; Kaufmann, M.; Créac'hcadec, R.; Vallée, T. Under Water Glued Stud Bonding Fasteners for Offshore Structures. *Int. J. Adhes. Adhes.* **2020**, *98*, 102533. https://doi.org/10.1016/j.ijadhadh.2019.102533.
7. Adhesive Bonding. In *Handbook of Plastics Joining*; William Andrew Inc.: Norwich, NY, USA, 2009; pp. 145–173. https://doi.org/10.1016/B978-0-8155-1581-4.50019-6.
8. Piekarczyk, M.; Grec, R. Application of Adhesive Bonding in Steel and Aluminium Structures. *Arch. Civ. Eng.* **2012**, *58*, 309–329. https://doi.org/10.2478/v.10169-012-0018-8.
9. Albiez, M.; Damm, J.; Ummenhofer, T.; Ehard, H.; Schuler, C.; Kaufmann, M.; Vallée, T.; Myslicki, S. Hybrid Joining of Jacket Structures for Offshore Wind Turbines—Validation under Static and Dynamic Loading at Medium and Large Scale. *Eng. Struct.* **2022**, *252*, 113595. https://doi.org/10.1016/J.ENGSTRUCT.2021.113595.
10. Romanos, G. Strength Evaluation of Axisymmetric Bonded Joints Using Anaerobic Adhesives. *Int. J. Mater. Prod. Technol.* **1999**, *14*, 430–444. https://doi.org/10.1504/IJMPT.1999.036282.
11. Yoneno, M.; Sawa, T.; Shimotakahara, K.; Motegi, Y. Axisymmetric Stress Analysis and Strength of Bonded Shrink-Fitted Joints Subjected to Push-Off Forces. *JSME Int. J. Ser. A* **1997**, *40*, 362–374. https://doi.org/10.1299/jsmea.40.362.
12. Sekercioglu, T. Shear Strength Estimation of Adhesively Bonded Cylindrical Components under Static Loading Using the Genetic Algorithm Approach. *Int. J. Adhes. Adhes.* **2005**, *25*, 352–357. https://doi.org/10.1016/j.ijadhadh.2004.11.002.
13. Sekercioglu, T.; Meran, C. The Effects of Adherend on the Strength of Adhesively Bonded Cylindrical Components. *Mater. Des.* **2004**, *25*, 171–175. https://doi.org/10.1016/j.matdes.2003.04.001.
14. Sekercioglu, T.; Gulsoz, A.; Rende, H. The Effects of Bonding Clearance and Interference Fit on the Strength of Adhesively Bonded Cylindrical Components. *Mater. Des.* **2005**, *26*, 377–381. https://doi.org/10.1016/j.matdes.2004.05.016.
15. Mengel, R.; Häberle, J.; Schlimmer, M. Mechanical Properties of Hub/Shaft Joints Adhesively Bonded and Cured under Hydrostatic Pressure. *Int. J. Adhes. Adhes.* **2007**, *27*, 568–573. https://doi.org/10.1016/j.ijadhadh.2006.11.003.
16. Aronovich, D.A.; Murokh, A.F.; Sineokov, A.P.; Khamidulova, Z.S. Study of the Properties of Anaerobic Adhesives Cured in Cylindrical Joints. *Polym. Science. Ser. D* **2008**, *1*, 260–265. https://doi.org/10.1134/S1995421208040102.
17. Sineokov, A.P.; Aronovich, D.A.; Murokh, A.F.; Khamidulova, Z.S. Mechanism of Initiation of the Curing of Anaerobic Adhesives. *Int. Polym. Sci. Technol.* **2008**, *35*, 31–38. https://doi.org/10.1177/0307174x0803500705.
18. Croccolo, D.; de Agostinis, M.; Vincenzi, N. Static and Dynamic Strength Evaluation of Interference Fit and Adhesively Bonded Cylindrical Joints. *Int. J. Adhes. Adhes.* **2010**, *30*, 359–366. https://doi.org/10.1016/j.ijadhadh.2010.03.003.
19. Croccolo, D.; de Agostinis, M.; Mauri, P.; Olmi, G. Influence of the Engagement Ratio on the Joint Strength of Press Fitted and Adhesively Bonded Specimens. *Int. J. Adhes. Adhes.* **2014**, *53*, 80–88. https://doi.org/10.1016/j.ijadhadh.2014.01.017.
20. Croccolo, D.; de Agostinis, M.; Vincenzi, N. Design and Optimization of Shaft-Hub Hybrid Joints for Lightweight Structures: Analytical Definition of Normalizing Parameters. *Int. J. Mech. Sci.* **2012**, *56*, 77–85. https://doi.org/10.1016/j.ijmecsci.2012.01.007.
21. Croccolo, D.; de Agostinis, M.; Fini, S.; Olmi, G. An Experimental Study on the Response of a Threadlocker, Involving Different Materials, Screw Dimensions and Thread Proportioning. *Int. J. Adhes. Adhes.* **2018**, *83*, 116–122. https://doi.org/10.1016/J.IJADHADH.2018.02.024.
22. Croccolo, D.; de Agostinis, M.; Fini, S.; Olmi, G.; Paiardini, L.; Robusto, F. Threaded Fasteners with Applied Medium or High Strength Threadlockers: Effect of Different Tightening Procedures on the Tribological Response. *J. Adhes.* **2020**, *96*, 64–89. https://doi.org/10.1080/00218464.2019.1679630.
23. Croccolo, D.; de Agostinis, M.; Fini, S.; Olmi, G.; Paiardini, L.; Robusto, F. Effects of Aging Temperature and Humidity on the Response of Medium and High Strength Threadlockers. *J. Adhes.* **2021**, *98*, 721–738. https://doi.org/10.1080/00218464.2021.1980393.

24. Croccolo, D.; de Agostinis, M.; Fini, S.; Olmi, G.; Paiardini, L.; Robusto, F. Temperature Response of LOCTITE 648 Anaerobic Adhesive and Hoop Channels to Enhance Its Effectiveness under High Interference. *J. Adhes.* **2021**, 1–25. https://doi.org/10.1080/00218464.2021.1986394.
25. Oinonen, a.; Marquis, G. A Parametric Shear Damage Evolution Model for Combined Clamped and Adhesively Bonded Interfaces. *Eng. Fract. Mech.* **2011**, *78*, 163–174. https://doi.org/10.1016/j.engfracmech.2010.10.003.
26. Oinonen, a.; Marquis, G. Shear Decohesion of Clamped Abraded Steel Interfaces Reinforced with Epoxy Adhesive. *Int. J. Adhes. Adhes.* **2011**, *31*, 550–558. https://doi.org/10.1016/j.ijadhadh.2011.05.002.
27. Hurme, S.; Oinonen, a.; Marquis, G. Fatigue of Bonded Steel Interfaces under Cyclic Shear Loading and Static Normal Stress. *Eng. Fract. Mech.* **2011**, *78*, 1644–1656. https://doi.org/10.1016/j.engfracmech.2011.02.006.
28. Kleiner, F.; Fleischmann, W. Technologies of Threadlocking and Interference-Fit Adhesive Joints. *Adv. Struct. Mater.* **2011**, *6*, 227–255. https://doi.org/10.1007/8611_2010_39.
29. Gallio, G.; Marcuccio, G.; Bonisoli, E.; Tornincasa, S.; Pezzini, D.; Ugues, D.; Lombardi, M.; Rovarino, D.; Fino, P.; Montanaro, L. Study of the Interference Contribution on the Performance of an Adhesive Bonded Press-Fitted Cylindrical Joint. *Int. J. Adhes. Adhes.* **2014**, *53*, 89–96. https://doi.org/10.1016/j.ijadhadh.2014.01.008.
30. Abdel Wahab, M.M. Fatigue in Adhesively Bonded Joints: A Review. *ISRN Mater. Sci.* **2012**, *2012*, 746308. https://doi.org/10.5402/2012/746308.
31. Dragoni, E. Fatigue Testing of Taper Press Fits Bonded with Anaerobic Adhesives. *J. Adhes.* **2003**, *79*, 729–747. https://doi.org/10.1080/00218460390214442.
32. Croccolo, D.; de Agostinis, M.; Vincenzi, N. How to Improve Static and Fatigue Strength in Press-Fitted Joints Using Anaerobic Adhesive. *Proc. Inst. Mech. Eng. Part C J. Mech. Eng. Sci.* **2011**, *225*, 2792–2803. https://doi.org/10.1177/0954406211411402.
33. Croccolo, D.; de Agostinis, M.; Vincenzi, N. Experimental Analysis of Static and Fatigue Strength Properties in Press-Fitted and Adhesively Bonded Steel–Aluminium Components. *J. Adhes. Sci. Technol.* **2011**, *25*, 2521–2538. https://doi.org/10.1163/016942411X580207.
34. Raghava, R.; Caddell, R.M.; Yeh, G.S.Y. The Macroscopic Yield Behaviour of Polymers. *J. Mater. Sci.* **1973**, *8*, 225–232. https://doi.org/10.1007/BF00550671.
35. Schlimmer, M. Anstrengungshypothese Für Metallklebverbindungen. *Materwiss Werksttech* **1982**, *13*, 215–221. https://doi.org/10.1002/MAWE.19820130606.
36. Chow, T.S. Stress–Strain Behavior of Polymers in Tension, Compression, and Shear. *J. Rheol.* **1998**, *36*, 1707. https://doi.org/10.1122/1.550281.
37. Zhang, J.; Jin, T.; Wang, Z.; Zhao, L. Experimental Investigation on Yield Behavior of PMMA under Combined Shear–Compression Loading. *Results Phys.* **2016**, *6*, 265–269. https://doi.org/10.1016/J.RINP.2016.05.004.
38. Spaggiari, A.; Castagnetti, D.; Dragoni, E. A Design Oriented Multiaxial Stress-Based Criterion for the Strength Assessment of Adhesive Layers. *Compos. Part B Eng.* **2019**, *157*, 66–75. https://doi.org/10.1016/j.compositesb.2018.08.085.
39. Castagnetti, D.; Dragoni, E. Predicting the Macroscopic Shear Strength of Adhesively-Bonded Friction Interfaces by Microscale Finite Element Simulations. *Comput. Mater. Sci.* **2012**, *64*, 146–150.
40. Castagnetti, D.; Dragoni, E. Experimental Assessment of a Micro-Mechanical Model for the Static Strength of Hybrid Friction-Bonded Interfaces. *J. Adhes.* **2013**, *89*, 642–659. https://doi.org/10.1080/00218464.2012.747179.
41. Castagnetti, D.; Dragoni, E. Adhesively-Bonded Friction Interfaces: Macroscopic Shear Strength Prediction by Microscale Finite Element Simulations. *Int. J. Adhes. Adhes.* **2013**, *53*, 57–64. https://doi.org/10.1016/j.ijadhadh.2014.01.016.
42. Castagnetti, D.; Dragoni, E. Experimental Investigation and Model Validation of the Shear Strength of Hybrid Interfaces up to Complete Failure. *J. Adhes.* **2016**, *92*, 679–697. https://doi.org/10.1080/00218464.2015.1115740.
43. Ragni, M.; Castagnetti, D.; Dragoni, E. Experimental Validation of a Simple Shear Strength Model for Hybrid Friction-Bonded Interfaces. *Int. J. Adhes. Adhes.* **2018**, *83*, 130–136. https://doi.org/10.1016/j.ijadhadh.2018.02.026.
44. Corigliano, P.; Ragni, M.; Castagnetti, D.; Crupi, V.; Dragoni, E.; Guglielmino, E. Measuring the Static Shear Strength of Anaerobic Adhesives in Finite Thickness under High Pressure. *J. Adhes.* **2019**, *97*, 783–800. https://doi.org/10.1080/00218464.2019.1704271.
45. Henkel Loctite® 243™, Technical Data Sheet 2010. https://www.henkel-adhesives.com/uk/en/product/threadlockers/loctite_243.html accessed on 1 July 2022.
46. Henkel Loctite® 638, Technical Data Sheet 2004, 80–82. https://www.henkel-adhesives.com/uk/en/product/retaining-compounds/loctite_638.html accessed on 1 July 2022.